Journal of Zhejiang University-SCIENCE A (Applied Physics & Engineering)
ISSN 1673-565X (Print); ISSN 1862-1775 (Online)
www.jzus.zju.edu.cn; www.springerlink.com
E-mail: jzus@zju.edu.cn

Review:

Design of suction foundations

Bas van DIJK
Fugro, 2631 RT, Nootdorp, The Netherlands
E-mail: b.vandijk@fugro.com

Received Aug. 30, 2017; Revision accepted Apr. 5, 2018; Crosschecked May 28, 2018

Abstract: Suction foundations have been deployed in the last three decades in a growing number of offshore developments, for bottom-fixed and floating structures, in shallow and deep waters, many of them successfully. Suction foundations, traditionally used as anchors and jacket foundations in the oil and gas industry, are now also used in the offshore renewable (wind) industry, e.g. for monopods, tripods, and jackets. When technically feasible, suction foundations are often cheaper than pile foundations. Additionally, their installation is relatively noise-free and, by applying overpressure, they can be removed during decommissioning. This paper focuses on the more complex design issues and some pitfalls related to suction foundation design. Additionally design practices and recommendations for suction caisson design, including installation and extraction feasibility, foundation resistance, settlements and response in sand, clay and layered soil profiles, will be presented for basic understanding.

Key words: Suction foundation; Caisson; Anchor; Bucket; Installation; Resistance, Capacity; Extraction
https://doi.org/10.1631/jzus.A1700465 **CLC number:** TU47

1 Introduction

Suction foundations are also called suction buckets, suction cans, suction anchors, suction piles or suction caissons. Although there are small perceptual differences, the different synonyms are all used in this paper, without distinction. The 'suction' term refers to the method used to install the foundation, i.e. using active suction by means of a pump. However, during the operational phase, passive suction is often relied upon for resistance. According to Tjelta (2015) active suction during the operational phase has been applied at the Gullfaks C platform, to accelerate the consolidation period of the soft soil at the site.

Suction foundations are "intermediate" foundations, in-between shallow foundations (L/D<0.2) and pile foundations (L/D>10), where L is the caisson installation depth (m) and D is the caisson diameter (m).

A suction foundation typically consists of a steel cylinder (skirt), closed at the top side (lid) in which suction can be applied by pumping water from the inside to the outside of the foundation, or vice versa, in case of extraction. Suction foundations are installed by self-weight penetration to a sufficient depth to start suction assisted penetration to the final penetration depth.

Suction foundations have been deployed in the last three decades in a growing number of offshore developments, for bottom-fixed and floating structures, in shallow and deep waters, many of them successfully. Tjelta (2015) presented an overview of the history of suction caissons, which began with testing and installation of 12 moorings in the late 1970s and beginning of 1980s by Shell at the Gorm field.

When feasible, suction foundations are often cheaper than piled foundations. By applying overpressure they can be fully removed, during installation (e.g. in case of excessive tilt), during relocation

ORCID: Bas van DIJK, https://orcid.org/0000-0002-8677-7667

or during decommissioning. Additionally, their installation is relatively noise-free. Many countries nowadays have strict noise emission limits to protect marine life, which require expensive noise mitigation measures and/or prohibit pile impact driving during a significant part of the year.

Although suction caissons are widely used, there are currently only a few standards related to suction caisson design. The few existing standards only cover parts of the full suction caisson design process. Moreover, the issues related to the design are changing, now that suction caissons are also used in the offshore wind industry. For example, long-term deformations, tilt, and dynamic response are typically important design situations in the wind industry, whereas capacity is dominating the design in the oil and gas industry.

2 Suction bucket installation feasibility

2.1 Theory

Installation feasibility checks usually consider the following aspects: (1) sufficient self-weight penetration to start the suction process; (2) avoidance of plug uplift (clay and layered clay-sand profiles) or soil liquefaction/piping (sand); (3) suction pressures not exceeding vacuum pressure.

During geotechnical design installation feasibility checks require the following assessments: (1) soil penetration resistance; (2) expected suction pressures; (3) plug uplift resistance (clay); (4) pressure at which piping or soil plug liquefaction occurs (sand); (5) vacuum pressure at the highest level of the suction system (usually at pump level).

Installation feasibility in sand only and clay only profiles is relatively well understood. Installation feasibility in layered soil profiles is more complex.

For sands and clays, two types of methods can be distinguished to assess the soil resistance: (1) classical bearing capacity methods and (2) cone penetration test (CPT)-based methods.

The classical bearing capacity equations for suction caisson penetration (without ground water flow) are:

sand profile:

$$R_t = q_{tip}A_{tip} + P_{si}\int f_{si}(z)\,\mathrm{d}z + P_{so}\int f_{so}(z)\,\mathrm{d}z, \quad (1)$$

$$q_{tip} = 0.5\gamma' tN_\gamma + qN_q, \quad (2)$$

$$f_{si} = \sigma'_{vi}K\tan\delta_i, \quad (3)$$

$$f_{so} = \sigma'_{vo}K\tan\delta_o; \quad (4)$$

clay profile:

$$R_t = N_c s_u A_{tip} + P_{si}\int f_{si}(z)\,\mathrm{d}z + P_{so}\int f_{so}(z)\,\mathrm{d}z, \quad (5)$$

$$f_{si} = \alpha_i s_{ui}, \quad (6)$$

$$f_{so} = \alpha_o s_{uo}, \quad (7)$$

where R_t is the total penetration resistance (kN), $A_{tip}=\pi Dt$, z is the depth below seafloor (m), K is the coefficient of lateral earth pressure (-), δ is the interface friction angle between sand and skirt wall (°), γ' is the submerged unit weight of soil (kN/m^3), t is the skirt wall thickness (m), q is the effective overburden pressure at tip level (kPa), s_u is the undrained shear strength (kPa), α is the adhesion factor between clay and skirt wall (-), σ'_v is the vertical effective stress (kPa), P_s is the perimeter of the skirt (m), N_c, N_γ, and N_q are bearing capacity factors (-) (Brinch Hansen, 1970), and the subscripts i and o represent the inner and outer skirts, respectively.

CPT-based methods relate the penetration resistance with CPT cone resistance q_c (kPa). A basic form (without ground water flow) for sand and clay is presented (DNV, 2017):

$$R_t = k_p q_c A_{tip} + (P_{si} + P_{so})\int k_f q_c(z)\,\mathrm{d}z, \quad (8)$$

where k_p is the empirical coefficient relating q_c to skirt tip resistance (-), and k_f is the empirical coefficient relating q_c to skirt friction (-).

Some methods, discussed in the sections below, provide most probable or best estimate (BE) and high estimate (HE) soil resistance, whereas other methods only provide BE soil resistance. The BE is the best estimate of the expected soil resistance, whereas the HE soil resistance is the value that is not expected to be exceeded. Where available, the HE is usually used to check installation feasibility. Normally high characteristic parameter values are selected for assessment of installation resistance. Usually a factor of safety of 1 is applied on the BE and HE soil resistance.

In some cases internal stiffeners will be used. Stiffeners and other contingency will add to the installation resistance of the caisson.

2.2 Installation in clay

2.2.1 Penetration resistance

Due to the impermeable nature of clay, there is practically no flow of groundwater during suction assisted penetration. As mentioned before, in practice two types of methods are used to determine the soil resistance: (1) classical bearing capacity methods such as those described in (Houlsby and Byrne, 2005a; DNV, 2005); (2) CPT-based methods such as that described in (DNV, 2017).

For the classical bearing capacity method (Eq. (5)), α is usually taken as the inverse of the clay sensitivity S_t (-) (DNV, 2005). Among others, Lee et al. (2005) back-analysed suction caisson installations in Gulf of Mexico and West Africa and found confirmation of this equation. For Gulf of Guinea soft clays, Colliard and Wallerand (2008) back-analysed α values between 0.1 and 0.26, which are, according to the authors, even lower than $1/S_t$.

The sensitivity of clay can be assessed by different test methods, such as laboratory vane (LV), unconsolidated undrained triaxial compression (UU), consolidated undrained triaxial test (CU), T-bar penetrometer, and ball penetrometer. Due to different ways of shearing and remoulding, these tests typically give different sensitivity values for the same clay. For the assessment of α, it is recommended to derive the sensitivity from the peak/remoulded UU tests or similar, which is usually roughly equivalent to the sensitivity derived from cyclic T-bar and ball penetration tests in clay.

DNV (2005) recommended using the direct simple shear (DSS) undrained shear strength as reference for the skirt friction component and the average of the triaxial compression, triaxial extension, and DSS undrained shear strength for the skirt tip component. This average value is usually also close to the DSS undrained shear strength.

Table 1 presents k_p and k_f empirical coefficients for the CPT-based methods in clay according to DNV (2017) for North Sea clays and Colliard and Wallerand (2008) for Gulf of Guinea soft clays.

Table 1 Empirical k_p and k_f coefficients in clay for CPT-based methods

Method	k_p	k_f
DNV (2017)		
Most probable	0.4	0.03
High expected	0.6	0.05
Colliard and Wallerand (2008)	0.4	0.006–0.018

2.2.2 Critical suction pressure

Plug uplift limits the suction pressure s (kPa) that can be applied. Plug uplift occurs when the suction force S (S=s×A_i, where A_i is the inner cross-sectional area of the suction bucket in m^2) is larger than the sum of the inner wall friction F_i (kN) and reversed end-bearing REB (kN) of the plug, assuming the weight of the soil inside the can cancels out with the soil weight outside the can. DNV (2005) recommended the use of a safety factor of 1.5 on the REB component.

Houlsby and Byrne (2005a) presented a method to calculate the maximum installation depth, taking into account the suction pressure, the reversed end-bearing, and the imbalance in vertical effective stress on the inside and outside of the suction caisson due to skirt friction on the inside and outside of the skirt. They estimated that the maximum installation depth in clay varies from 3×D for stiff clays to 6×D for normally consolidated clays. They noted that some prototype installations achieved larger installation depths than those mentioned above, and hence the values can be treated as conservative.

2.3 Installation in sand

2.3.1 Penetration resistance

Suction pressures during installation in sand initiate groundwater flow. On the outside of the caisson, the groundwater flow causes a reduction in water pressure and an increase in effective stress, and hence an increase of the friction on the outer skirt wall. At the tip and on the inside of the caisson suction, the groundwater flow reduces the effective stress resulting in a reduction of the friction on the inner skirt wall and a reduction of the tip resistance, when compared to a no flow condition.

The flow conditions depend on the permeability of the soil in the vicinity of the suction bucket. Impermeable layers (e.g. clay) near the suction bucket

tip and spatial variability of the permeability may influence the flow conditions and hence the changes in effective stress. The water flow and effective stress may also result in a change in (relative) density and permeability of the soil plug (Tran et al., 2005). According to Erbrich and Tjelta (1999), Houlsby and Byrne (2005b), Tran et al. (2005), and Andersen et al. (2008), the permeability of the soil plug may increase during installation by a factor k_r (-) varying between 1 and 3, where k_r is the ratio between the permeability of the sand inside the caisson and the sand outside the caisson (-). Erbrich and Tjelta (1999) and Houlsby and Byrne (2005b) reported k_r values between 2 and 3, based on back-analysis of prototype installations. Tran et al. (2005) reported k_r values between 1 and 2, with an average of 1.5 based on results of centrifuge tests.

As for clays, in practice two types of methods are used to determine the soil resistance in sand: (1) classical bearing capacity methods such as described by Houlsby and Byrne (2005b) and Andersen et al. (2008); (2) CPT-based methods such as described by Senders and Randolph (2009) and DNV (2017).

The classical bearing capacity methods require estimation of the coefficient of lateral pressure K (-). Measurement of K is difficult and usually has a high degree of uncertainty. Usually K is assessed by CPT correlation. Furthermore, according to Broug (1988), K varies with changes in vertical effective stress.

The Houlsby and Byrne (2005b), Andersen et al. (2008), and Senders and Randolph (2009) methods include effects of water flow on the installation resistance. Houlsby and Byrne (2005b) also considered the increased effective stress on the inside and outside of the skirt due to skirt friction. In their theoretical model, the friction effect increases the vertical effective stress, which is redistributed by a load spread factor (i.e. the diameter of the area over which the load is spread versus depth, which they assumed to be 1 on the inside and outside of the skirt, based on back-analysis of several cases). The increased vertical effective stress also increases the end-bearing component. The increased vertical effective stress linearly increases inner and outer frictions (as K is kept constant). The effect was studied by the author by comparing the Houlsby and Byrne (2005b) method with the increased vertical effective stress due to the friction effect (without suction pressures) with a simple finite element method (FEM) model using a commercially available program (Fig. 1). In the axisymmetric model, a (wished in place) vertical skirt (plate) was pushed into (dense) sand without suction, until failure. The sand was modelled using a Mohr Coulomb model. The skirt-soil interface shear stress in the FEM model increases rapidly near seafloor, probably due to rotation of stresses. After the rapid increase near seafloor, it shows a lower increase with depth compared to the Houlsby and Byrne (2005b) model. Although probably not correct either, the FEM calculation shows that the stress state during suction caisson penetration is probably more complex than assumed in the theoretical model by Houlsby and Byrne (2005b).

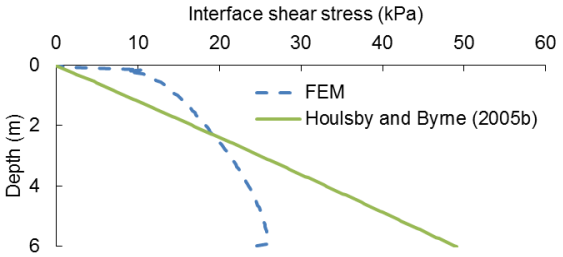

Fig. 1 Interface shear stress near the outer suction caisson skirt during installation in sand

The DNV (2017) method is for calculation of skirt penetration without suction (for skirted gravity base structures). The DNV (2017) method requires correction for the effect of water flow on the resistance. The change in effective stress due to water flow will lead to a change in cone resistance. This will lead to an increase of outer skirt skin friction and a decrease of inner skirt skin friction and skirt end-bearing. This can be assessed by principles as outlined by Houlsby (1998), Erbrich and Tjelta (1999), and/or Andersen et al. (2008). It can be inferred that the effect of increased effective stresses adjacent to the skirt due to skirt friction and in turn its effect on the skirt resistance is included in the calibration of the k_f and k_p factors in the DNV (2017) method. This means that this effect does not need to be considered for the CPT-based methods.

Houlsby and Byrne (2005b) considered the effect of flow on the effective stresses in the soil and adjusted the outer and inner skirt friction and end-bearing components accordingly. This approach

resulted in a linear change in cone resistance for the DNV (2017) method, as also recommended by ISO (2016) for scour effects when using CPT-based pile capacity methods.

However, the cone resistance is dominated by the horizontal effective stress and does not vary linearly with change in vertical effective stress (Begemann, 1976; Broug, 1988). Broug (1988) presented a method to assess the change in horizontal stress due to changes in vertical effective stress, based on experiences with CPT measurements at excavations.

For their classical bearing capacity model, Andersen et al. (2008) considered stress increase only for the skirt tip resistance due to the skirt friction, but did not adjust the inner and outer skirt friction components themselves. Their back-calculated K values showed significant variation, between 0.8 for prototypes and up to 1.85 for laboratory and field model tests, where 0.8 is the recommended value for design.

Erbrich and Tjelta (1999) considered a change in skirt friction along the caisson inner skirt. They suggested reducing the inner friction by a factor presented in Eq. (9). The factor was derived from finite element analysis.

$$\frac{f_{s;red}}{f_{s;unred}}=\left(\frac{1}{1-i_i}\right)^{\sin\varphi'}(1-i_i), \tag{9}$$

where $f_{s;red}$ is the reduced internal skirt friction, due to suction (kPa), $f_{s;unred}$ is the internal skirt friction without suction (kPa), i_i is the average internal gradient between the skirt tip and base plate (-), and φ' is the angle of internal friction (°). It is noted that Eq. (9) is not very sensitive to φ'. Erbrich and Tjelta (1999) did not give details for assessment of the outer skirt friction and skirt tip resistance.

Fig. 2 illustrates the effect of reducing the inner skirt friction of the DNV method for water flow by Broug (1988), Erbrich and Tjelta (1999), and Houlsby and Byrne (2005b) methods for arbitrarily chosen soil parameters for very dense sand. The method by Broug (1988) gives results similar to that by Erbrich and Tjelta (1999). The Houlsby and Byrne (2005b) method results in the largest reduction. As will be seen in examples below, the difference in resulting required suction pressure between the three methods is relatively small.

Table 2 presents k_p and k_f empirical coefficients for the CPT-based methods according to DNV (2017), Andersen et al. (2008), and Senders and Randolph (2009). Table 2 indicates a significant range in the empirical coefficients, especially for the k_p coefficient.

The reduction in inner skirt fiction and end-bearing is related to the reduction in effective stress, which in turn is related to the flow induced pore water pressure.

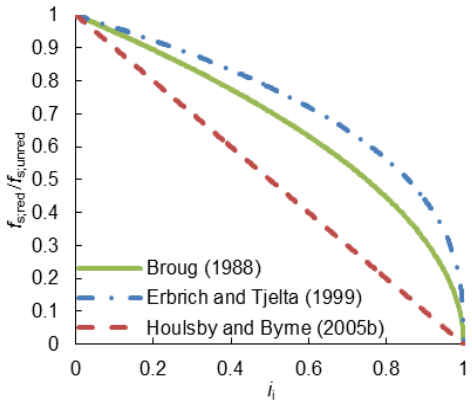

Fig. 2 Internal skirt friction

Table 2 Empirical k_p and k_f coefficients in sand for CPT-based methods

Method	k_p	k_f
DNV (2017)		
Most probable	0.3	0.001
Highest expected	0.6	0.003
Andersen et al. (2008)	0.01–0.6	0.001–0.0015
Senders and Randolph (2009)	0.2	0.0018–0.0026*

* $k_f=0.12\left[1-\left(D_i/D_o\right)^2\right]^{0.3}\tan\delta$

Houlsby and Byrne (2005b) defined the ratio of excess pore pressure at tip of caisson skirt to seafloor as a (-). They performed finite element analyses to derive values of a in a soil of uniform permeability for a thin-walled caisson for values of z/D up to 0.8 and for different values of k_r. Based on the finite element analyses they found the following equation for a, capturing the trend of the calculations reasonably well:

$$a=\frac{a_1k_r}{(1-a_1)+a_1k_r}, \tag{10}$$

$$a_1 = 0.45 - 0.36\left[1 - \exp\left(-\frac{z}{0.48D}\right)\right]. \qquad (11)$$

Tran and Randolph (2008) conducted a series of centrifuge tests to investigate the variation of suction pressure as function of self-weight surcharge, during installation in dense sand. Fig. 3 presents results from selected tests. The measured normalised pressure reduction due to a load increase of 490 kN or 50 metric tons ($\Delta s/(\gamma' D)$) is approximately 0.05, whereas the additional load, expressed as $\Delta s/(\gamma' D)$ is about $(50/A_i)/(\gamma' D)$=0.3. Hence, a change in (self-weight) load on the suction bucket has only a limited effect on the required suction pressure. The reason is that the resistance changes due to the change in suction. This effect is more significant than the change in load.

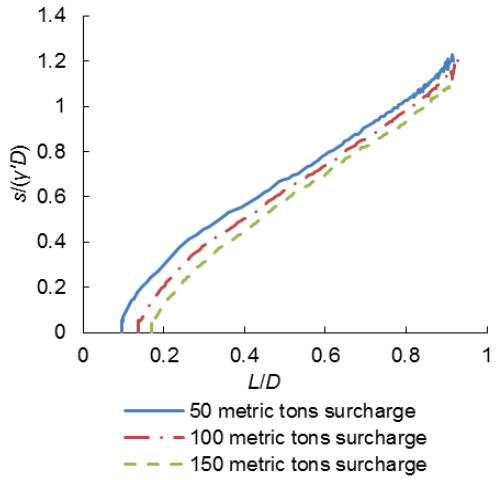

Fig. 3 Installation with surcharges of 50, 100, and 150 metric tons. Reprinted from (Tran and Randolph, 2008), Copyright 2008, with permission from ICE Publishing

Fig. 4 presents suction caisson installation data measured at four sites consisting of sand profiles. The figure also includes results from four prediction methods: (1) Andersen et al. (2008); (2) Senders and Randolph (2009); (3) DNV (2017) with the effect of water flow using principles of Houlsby and Byrne (2005b); (4) DNV (2017) with the effect of water flow using principles of Broug (1988).

The presented predictions use BE soil parameter values selected by the author. Thus, results may differ from those presented in other papers. From Fig. 4, the following observations can be made:

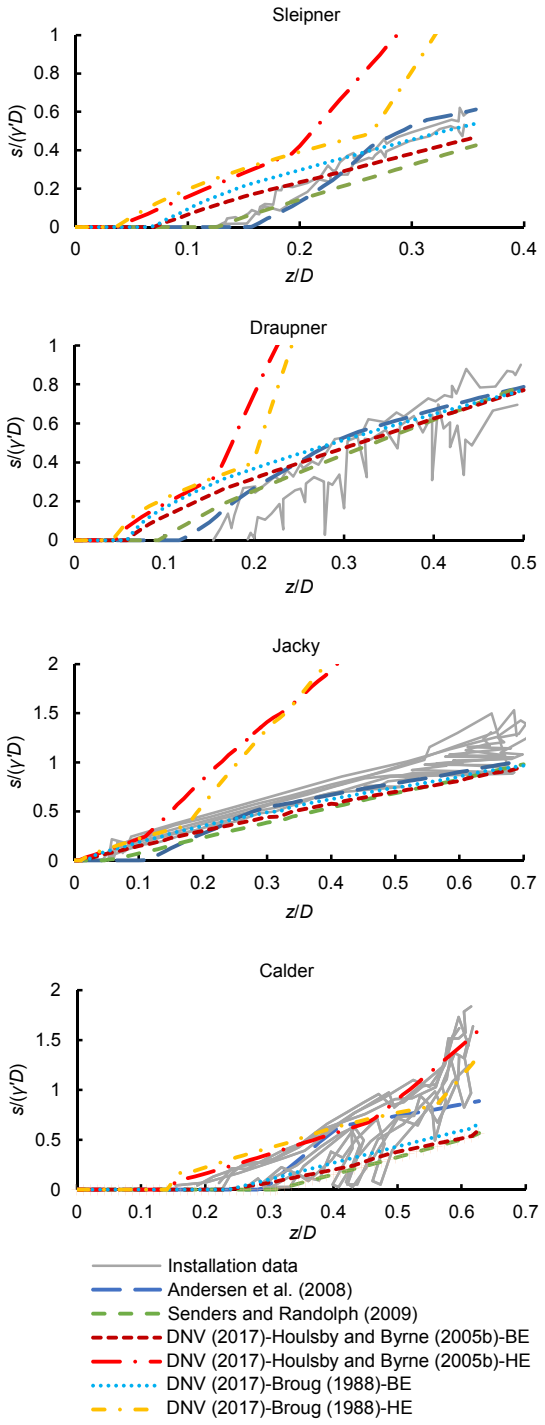

Fig. 4 Measured and predicted suction pressures

1. Measured suction pressures at each location show significant variation.

2. All prediction methods provide approximate indication of suction pressures; none provide consistently good predictions. Part of the difference might be due to uncertainties in parameter selection,

spatial variability of soil conditions and/or self-weight load on the individual suction buckets. Similar uncertainties exist during design and should be considered in parameter selection for design.

3. The HE methods can be regarded as design methods, with intrinsic caution. Nevertheless, the measured suction pressures for the Calder structure are locally higher than the HE value.

4. The HE of the DNV method shows a distinct change in suction pressure, with increasing z/D, for all four locations. Such change was not observed at the Sleipner, Draupner, and Jacky locations. At the Calder location, the measured data suggest a trend similar to the DNV HE method. For the DNV methods this distinct change happens when the suction pressure is equal to the critical suction pressure. At that moment, the internal friction and end-bearing reduce to 0 kN and cannot further reduce in the calculation model.

2.3.2 Critical suction pressure

Current state of design practice defines the critical hydraulic gradient i_{crit} (-) in sand at which piping or liquefaction will occur as

$$i_{crit}=\frac{\gamma'}{\gamma_w}, \tag{12}$$

where γ_w is the unit weight of water (kN/m^3).

A distinction can be made between the average hydraulic gradient from the skirt tip to the top of the soil plug, as suggested by Erbrich and Tjelta (1999) and Houlsby and Byrne (2005b) and the exit hydraulic gradient at seafloor inside the suction caisson, as suggested by Feld (2001), Andersen et al. (2008), and Senders and Randolph (2009). The latter is usually higher.

Among others, models for the critical suction pressure s_{crit} (kPa), have been proposed by Erbrich and Tjelta (1999), Feld (2001), Houlsby and Byrne (2005b), Andersen et al. (2008), Senders and Randolph (2009), and Ibsen and Thilsted (2010), presented in Fig. 5. These models are mainly based on finite element analysis. Erbrich and Tjelta (1999) and Houlsby and Byrne (2005b) considered a change in permeability of the sand inside the caisson. As mentioned in Section 2.3.1, literature indicates that the k_r value ranges between 1 and 3. Erbrich and Tjelta (1999) also considered a case where only the permeability in a zone of 0.07×D adjacent to the skirt wall was increased. The Houlsby and Byrne (2005b) method and the Erbrich and Tjelta (1999) method for k_r=1 and the Andersen et al. (2008) method for k_r=3 encompass the other models.

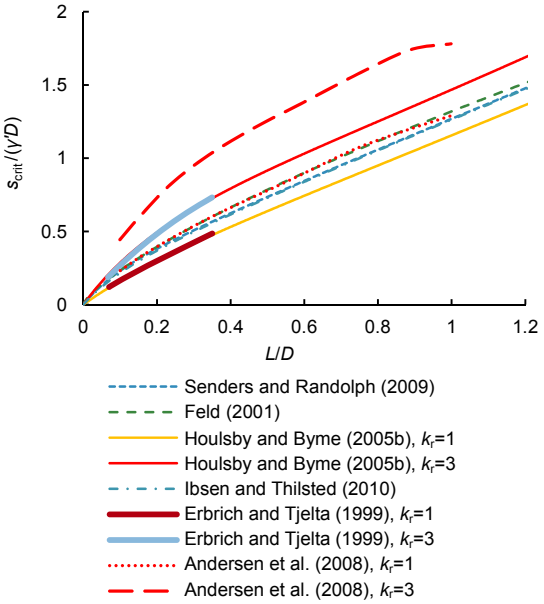

Fig. 5 Critical suction pressure

Usually the maximum achievable penetration depth using these models is approximately equal to the suction bucket diameter (Houlsby and Byrne, 2005b).

Experiences from model tests showed that very large internal gradients are nearly always required to cause skirt penetration, but unless deliberately provoked, extensive soil heave or piping does not occur (Erbrich and Tjelta, 1999). Andersen et al. (2008) reached the same conclusions based on prototype and model tests.

Panagoulias et al. (2017) studied installation data and model tests available in the public domain. They found that, for many installations of suction caissons in dense to very dense sand, measured suction pressures s (kPa) exceeded the theoretical critical suction pressure as predicted by the above mentioned models for k_r values up to 3. Fig. 6 presents predicted critical suction pressure and measured suction pressure, which lie above the critical suction pressure. The figure presents some of the results from Panagoulias et al. (2017). Panagoulias et al. (2017) also carried out laboratory upward flow tests (LUFT), using a standard permeameter. The experiments indicated that the

higher suction pressures may be attributed to soil arching inside the suction caisson, but that soil arching may not occur for: (1) very loose to medium dense sand; (2) possibly for small L/D ratios; (3) possibly for uniform sand. Soil arching is the transfer of pressure from yielding soil masses onto adjoining stationary parts by shear resistance, reducing the pressure on the yielding part and increasing the pressure on the stationary part (Terzaghi, 1943). It is recommended, if soil arching is not expected to occur, not to exceed the critical suction pressure assessed with the models presented above.

The installation of suction (mooring) anchors in the Gorm field indicated that indeed there is a limit to the suction pressure. During the installation of the mooring anchors, a plug heave of up to 2.6 m occurred (Senpere and Auvergne, 1982). The diameter of the suction buckets was 3.5 m and the installation depth 8.5 m to 9 m. With a soil profile consisting of clay overlain by 5 m to 7 m medium dense to dense sand, the installation depth in the top sand layers was equal to 1.5 to 2 times the suction bucket diameter. Hence, it is likely that the critical suction pressure was exceeded, leading to piping and/or plug liquefaction. It is noted that the self-weight of the suction buckets was compensated by the crane. However, this change in load is expected to have a small effect as shown by Tran and Randolph (2008).

It was concluded that soil arching may lead to higher critical suction pressures than predicted by current models. However, further research is recommended into the actual critical suction pressure to be allowed.

No safety factors are usually applied on the critical suction pressure, although for installation feasibility assessments, when using CPT-based methods, normally a high estimate soil resistance case is considered.

2.4 Installation in layered soils

2.4.1 Penetration resistance

The penetration resistance in layered soils can be assessed by summing the separate resistance components for the clay and sand layers.

If sand is overlain by clay, the clay layer will prevent groundwater flow. Limited penetration may be possible into the sand layer. When the suction pressure is increased beyond the critical suction pressure, two mechanisms can occur (Senders et al., 2007):

1. Water seepage along the skirt and/or through cracks in the clay layer, where the cracks may have been formed because of the suction pressure. Water will flow through the cracks, which will result in a "suction" pressure in the sand layer below the clay layer, resulting in a reduction in inner skirt skin friction and skirt end-bearing resistance.

2. Uplift of the clay plug, reducing the vertical effective stress of the sand layer below. When increasing the suction pressure, the effective stress at the top of the sand layer reduces ultimately to zero. If the suction pressure is increased further, the clay plug will move upwards, whereas the sand will not move, inducing a water flow in the sand and a water filled gap between the clay and sand layer. After installation, due to self-weight and operational loads, the water gap can disappear, causing foundation settlement. Whether this settlement can be allowed or not depends on the design criteria.

Senders et al. (2007) presented a method for assessing the penetration resistance during suction caisson installation in a clay over sand profile. In order to limit the water-filled gap for the second mechanism, they recommended fast installation (i.e. high pumping rate).

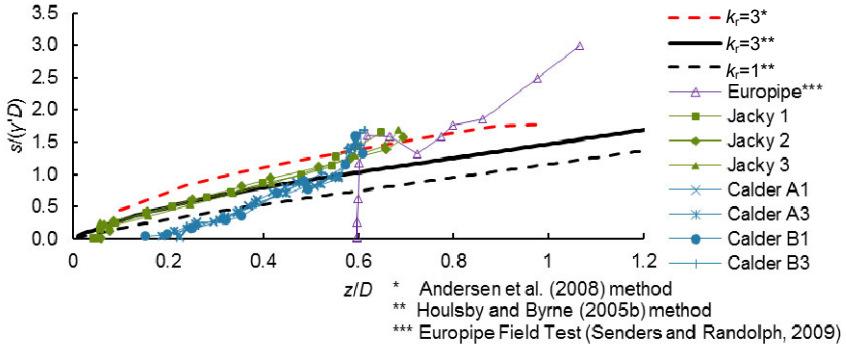

Fig. 6 Measured suction pressures versus theoretical suction pressures

Watson et al. (2006) performed centrifuge tests of suction caisson installation in layered profiles, consisting of ca. 37 mm of clay (ca. 5.6 m 150*g*, where *g* is the gravitational constant of 9.8 m/s^2), overlain by ca. 11 to 18 mm sand (ca. 1.6 to 2.7 m at 150*g*) and underlain by very dense sand. The target installation depth was ca. 62 mm (9.3 m at 150 *g*) and the suction caisson diameter was 80 mm (12 m at 150*g*). Test results are presented in Table 3 and in Fig. 7. The suction caissons were jacked to a total load varying between 140 and 360 N. After that suction was applied. The increase in the total load between 50 and 55 mm penetration indicates the depth of the top of the lower dense sand layer for each test. In tests S4-2 and S4-5 significant plug lift occurred (3 mm and 5 mm, respectively; ca. 0.45 to 0.75 m at 150*g*) and the penetration stopped at a reduced penetration depth. The tests prove that, in this particular case, installation of about 1.1 m into a very dense sand layer overlain by a clay layer is achievable.

Tran et al. (2007) performed centrifuge tests of suction caisson installation in sand with a 1 m thick silt layer (at 100*g*). They observed a sharp increase in suction pressure when the suction bucket penetrated from the sand layer into the silt layer (Fig. 8), followed by a drop in suction pressure while the caisson was still penetrating into the silt layer. The sharp increase is thought to be caused by the decreased flow of groundwater through the less permeable silt layer. Tran et al. (2007) believed that the drop in suction pressure above sand layers can be explained by uplift of the silt due to the suction pressure. Penetration into a lower sand layer below the silt layer led to a higher suction pressure gradient with depth, compared to a homogeneous sand profile (Fig. 8). The gradient is caused by the less permeable silt layer that blocks flow of groundwater.

Table 3 Test results

Test	Thickness of top sand layer (mm)	Depth to very dense sand (mm)	Penetration into very dense sand (mm/m*)
S4-2	13.0	50.0	9/1.4
S4-3	17.0	54.0	7/1.1
S4-4	18.0	55.0	6/0.9
S4-5	11.0	48.0	8/1.2
S4-6	17.5	54.5	7/1.0

* Penetration at 150*g*. Data from (Watson et al., 2006)

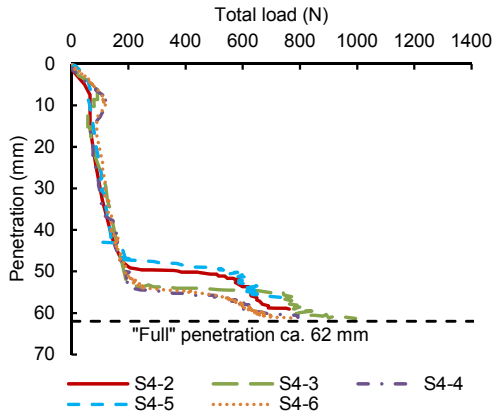

Fig. 7 Centrifuge suction caisson installation tests in layered ground profiles. Reprinted from (Watson et al., 2006), Copyright 2006, with permission from Taylor & Francis Books UK

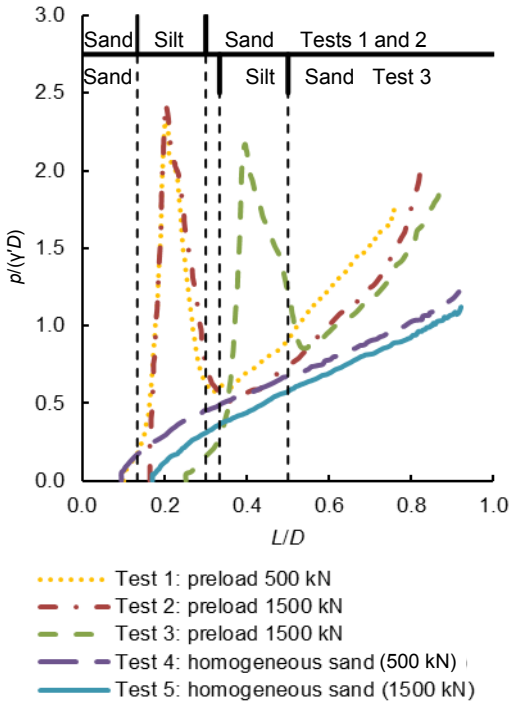

Fig. 8 Suction pressures measured in sand with silt layers. Adapted from (Tran et al., 2007), Copyright 2007, with permission from ASCE

Allersma et al. (2001) presented an alternative installation method, referred to as 'percussion method'. This method considers a depression tank added to the pumping system. A vacuum pressure is created in the tank. During penetration in sand overlain by clay, a crossover valve is opened, causing a (temporary) abrupt pressure drop inside the caisson. This process is repeated until the caisson has fully penetrated into

the soil. According to the authors, this method substantially reduces the risk of penetration refusal in sand. The method was tested in centrifuge tests, in sand, clay and layered soils and has been successfully applied for a real structure.

If a clay layer is overlain by a sand layer, the influence of the approaching clay layer on the flow in the sand layer needs to be taken into account. Ibsen and Thilsted (2010) presented an empirical expression for assessment of the suction pressure during installation in a sand over clay profile, based on curve fitting with calculations with a finite difference program for different embedment depths over diameter ratios and thickness of the top sand layer over diameter ratios. The assessment of the suction pressure in the clay layer below a sand layer is similar to that for a clay only profile.

2.4.2 Critical suction pressure

Ibsen and Thilsted (2010) presented a model to assess the critical suction pressure during installation in a sand over clay profile. The model is based on combining the curve fitting empirical equation (Section 2.3.2) with Eq. (12).

2.5 Plug heave

Plug heave may occur due to the skirt displacing the soil. Cautiously, it can be assumed that half of the displaced soil goes into the suction caisson when the suction bucket penetrates under self-weight and all the displaced soil goes into the suction caisson when suction is applied. It can be expected that the displaced soil will not be evenly distributed at seafloor, but will be more concentrated near the skirt. The distance from the skirt over which the displaced soil is distributed depends mainly on the diameter and skirt length and can be estimated by a geotechnical expert using engineering judgement or by large deformation finite element analysis.

In sand, additional plug heave may occur due to a reduction in density of the soil plug. As mentioned before, the reduction in density of the soil plug is caused by ground water flow and shear stress due to skirt penetration.

To account for plug heave usually the skirt length is extended with the expected plug heave and an additional margin. Moreover, foundation design may require the caisson skirt to penetrate so that the top of the plug is at the level of the lid, although often under base grouting is considered. Hence, if the plug heave is less than expected, the skirt may need to penetrate deeper (i.e. beyond the depth necessary for capacity).

2.6 Difficult ground conditions

Although suction caissons are used in a wide range of soil conditions, there are also challenging soil conditions for suction caisson installation.

Soils containing large boulders, such as drop stones, can lead to foundation tilt, refusal during installation, and damage to the skirt tip. A possible remedial measure is to de-install the suction caisson and re-install at a different location.

If the self-weight penetration is insufficient (i.e. too shallow to form a sufficient seal), the suction installation process cannot be started. Seafloor undulations can lead to differences in self-weight penetration depth and gaps along the caisson perimeter.

Gravel layers may be difficult to penetrate, especially if present at or near seafloor. They may limit the self-weight penetration. Moreover, their high permeability can prevent the suction pressure to build up.

2.7 Pump capacity

The required pump capacity depends on the required installation speed and, for foundation installation in sand, water seepage through the soil. Typical installation speeds vary between 0.02 to 0.1 m/min. The seepage in sand can be assessed using Darcy's law, giving consideration to the possible effect of a change in permeability due to the suction process inside the suction caisson.

The capacity of centrifugal pumps depends on the pressure difference. A higher pressure difference will lead to a lower capacity, and vice versa. Pump selection should consider that the required capacity can be achieved at the required pressure difference.

In shallow water depths, the pump should be placed close to the lid of the caisson. This position maximises achievable pressure difference.

3 Suction foundation resistance

3.1 Theory

Suction foundations can resist vertical V_a (kN),

horizontal H_a (kN), moment M_a (kNm), and torsional T_a (kNm) actions. Torsional actions are often small. The resistance of a suction bucket for undrained conditions has a conical shape in vertical-horizontal-moment (VHM) space (Fig. 9). Although suction buckets have a relatively high rotational resistance M (kNm), they are usually more efficient (i.e. smaller and more cost effective) if the moment actions are reduced at the point of rotation by means of a stronger connection to the supporting super-structure (e.g. jacket) or by a connection near the point of rotation (e.g. anchor lug). In case of a potential for a gap at the back of an anchor due to loading, it may be beneficial to locate the lug at a lower point to mitigate the formation of a gap. Eliminating the moment action (M_a=0 kNm) of a suction anchor at the point of rotation gives the highest vertical-horizontal (VH) resistance and the smallest bucket size. Similarly eliminating M_a at the point of rotation of the suction caisson, by creating a "moment fixity" between the suction caisson top lid and the jacket structure, will result in an increase in VH resistance whereas this usually only leads to a small increase in V_a (depending on the distance between the suction caissons). This usually leads to the smallest suction caisson size; however, it is a trade-off between suction caisson size and an increase in steel to provide a stronger connection between the suction caisson top plate and the jacket structure.

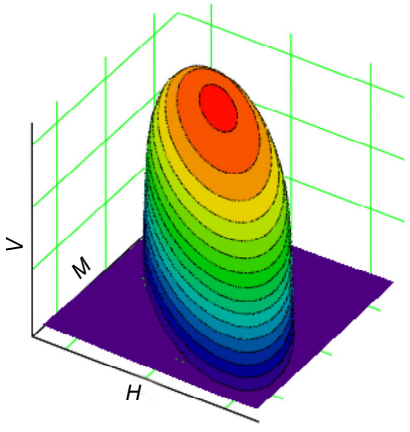

Fig. 9 VHM resistance envelope for undrained conditions

As will be discussed in the following sections, some suction caisson designs rely on the undrained tensile capacity of a suction bucket, where a suction pressure may occur between the top lid of the suction bucket and the soil directly underneath. Depending on the water depth, there is the possibility of a limiting resistance, due to a vacuum pressure occurring below the suction caisson lid.

Design situations for suction caissons are generally similar to other foundation types. Consideration should be given to changes in site conditions during the design life of the structure. Particularly, this includes consideration of soil scour and deposition around a suction foundation and consideration of shallow gas accumulation inside a suction foundation (Gylland and de Vries, 2008). Furthermore, trenching issues may occur, such as encountered along the anchor chain of the Serpentina floating production, storage, and offloading (FPSO) vessel (Fig. 10). The suction anchor was installed in a clay profile. According to Bhattacharjee et al. (2014) the trench was primarily caused by significant motion of the ground chain. Obviously, such trenches decrease the capacity of the suction caisson. For the Serpentina FPSO mooring it was decided to replace the existing anchors with gravity-installed anchors with a 30% increased anchor radius. O'Neill et al. (2018) presented a method to predict the primary mechanism behind trench formation induced by anchor chain motions. Fig. 11 shows the back-analysis of the Serpentine FPSO trenches using this model where soil strength (low estimate (LE) soil and HE soil), water depth ds (m), total chain length Lc-t (m), and fairlead horizontal distance from the padeye at pretension xa-s (m) were varied. They concluded that the primary mechanism behind trench formation is the remoulding and reworking of the soil as a result of continual horizontal line movements, which they believed to be the critical mechanism for assessing whether trenching will occur or not. The secondary trench formation mechanisms, which cause additional excavation, are more prevalent when the mooring line is slackened off, with repeated cycles of contact between the underside of the chain and the soil which causes remoulding suspension and erosion of particles. Trenching is most likely to occur for semi-taut to taut mooring configurations particularly when embedded in soils with relatively low strength.

3.2 Resistance in clay

For sustained actions, such as self-weight, clay will initially behave undrained. Due to consolidation,

the behaviour will change to drained conditions with time. For short-term actions, such as waves during a storm, the behaviour is usually considered as undrained during the entire storm.

The undrained VHM resistance of a caisson in clay can be assessed using (a) resistance envelopes such as developed by Kay and Palix (2010, 2011), Kay (2013), and van Dijk (2015), (b) limit equilibrium analysis such as presented by Kolk et al. (2001), and/or (c) the upper bound of plasticity such as developed by Murff and Hamilton (1993). The resistance envelopes are based on a large number of finite element analysis (FEA) for several schematic undrained shear strength s_u (kPa) profiles. The results of the FEA are curve fitted by rotated ellipsoids and normalised by L, D, and s_u. This makes them applicable to a large range of geometries and s_u profiles. They encompass the range of L/D from 0.1 to 6 and the range of $e_{z,su}/L$ of 0.5 to 0.75, covering many clay profiles found offshore, where $e_{z,su}$ is the geometric centre of gravity of the s_u profile below seafloor. The methods assess the geometric centre of gravity of the s_u profile $e_{z,su}$ (m) below seafloor. For example, this results in an $e_{z,su}/L$ of 0.5 for a constant s_u and an $e_{z,su}/L$ of 2/3 for a linearly increasing s_u profile from 0 kPa at seafloor. It seems reasonable to calculate $e_{z,su}/L$ for other s_u profiles (i.e. different from the schematic profiles) and interpolate between the values found for the schematic profiles. The VHM resistance envelopes methods exclude a model for maximum vertical bearing resistance V_{max}. V_{max} can be assessed using conventional bearing capacity equations for end-bearing and skirt frictional resistance. During penetration, the clay will remould. Hence, initially the skirt frictional resistance will be low, but it will increase with time due to thixotropy. Additionally due to lateral loading, a gap may form on the outside of the suction caisson. A gap may significantly reduce the suction caisson capacity. A gap would only be expected if the clay is sufficiently strong and if the lateral loads are sufficiently high such that the bucket foundation mobilises significant plastic lateral deformation.

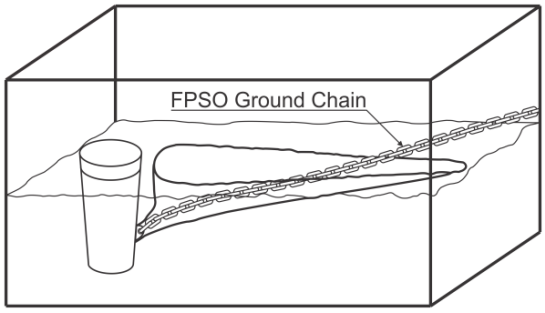

Fig. 10 Trenching in front of suction anchor. Adapted from (Bhattacharjee et al., 2014), Copyright 2014, with permission from Offshore Technology Conference (OTC). Further reproduction prohibited without permission

The undrained shear strength of clay can deteriorate when cyclically loaded, e.g. due to wave loading. Fig. 12 shows the schematisation of gradual wave

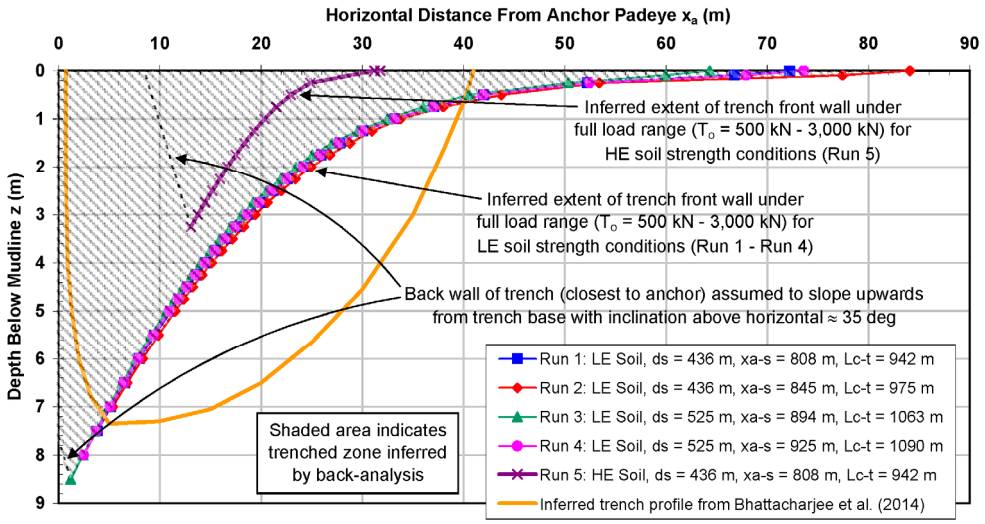

Fig. 11 Back-analysis of Serpentina FPSO mooring line trench using the primary mechanism of trench formation. Reproduced from (O'Neill et al., 2018), Copyright 2018, with permission from Offshore Technology Conference (OTC) Further reproduction prohibited without permission

height built-up during a design storm, which can be used to derive a cyclic load history, where H_s is the wave height (m) and H_{smax} is the maximum wave height (m) during a design storm.

Another method is to transform the site specific, irregular cyclic wave load history into parcels of constant cyclic loads (Fig. 13), for example, using the method described by Hansteen (1981). Hansteen (1981) developed tables with wave height and numbers of cycles for different design storms according to this approach. These tables and results of laboratory cyclic triaxial (TA) and DSS tests allow calculation of pore pressure accumulation (Andersen, 2015) to derive cyclic undrained shear strengths for a design storm, where F is the load (kN), F_{max} is the maximum load (kN) during a storm, and N is the number of cycles.

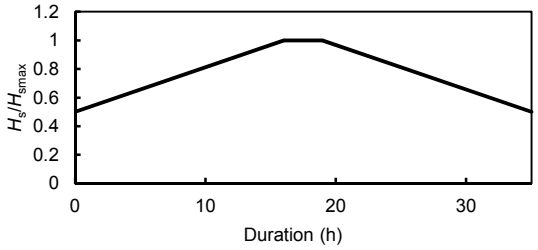

Fig. 12 Wave height build-up during a storm. Adapted from (Norsok, 2017), Copyrights 2017, with permission from Society of Petroleum Engineers

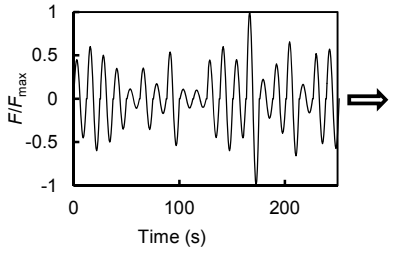

N	F/F_{max}
1	100
2	95
4	88
8	81
15	74
30	67
50	59
90	51
200	41
500	23

Fig. 13 Transformation of cyclic load history into load parcels (data in the table is from (Hansteen, 1981))

The pore pressure accumulation procedure is presented in Fig. 14. One of the assumptions of the method is that the shear stresses are proportional to the loads. Pore pressure accumulation is determined (upper graph) for different normalised shear stress ratios τ_{cy}/σ'_{vc}, where τ_{cy} is the cyclic shear stress (kPa) and σ'_{vc} is the vertical consolidation pressure (kPa). The locus of end points can be copied onto the strain contour diagram (lower graph). For the maximum allowable strain (e.g. 15%), the cyclic shear strength ratio $\tau_{cy,f}/\sigma'_{vc}$ (-) and the equivalent number of cycles to failure $N_{eq,f}$ (-) can be assessed, where $\tau_{cy,f}$ is the cyclic shear strength at failure (kPa). Another method is the strain accumulation procedure (Andersen, 2015), where the accumulated strain is used to assess the cyclic strength degradation, instead of accumulated pore pressures.

The average shear stress τ_{av} (kPa) is important, as the cyclic shear strength depends on τ_{av}. Usually two-way loading (i.e. when $|\tau_{av}|<\tau_{cy}$) is more destructive than one-way loading (i.e. when $|\tau_{av}|>\tau_{cy}$).

A distinction can be made between the shear strength in compression, the shear strength in extension and for DSS, both for monotonic and cyclic loading conditions. Depending on the loading conditions all three types of shear strength can be present. It is often reasonable to consider the average of the three types of shear strength, which is usually close to the DSS shear strength.

The pore pressure accumulation approach relies on data from laboratory testing of sampled soil. It can suit direct use in calculation models that require BE input parameters derived from laboratory tests without correction for undisturbed sample quality and strain compatibility. However, note that stress-strain measurements for laboratory test specimens will not be fully representative of in situ conditions. If a calculation model requires correction, then common options available to a designer are (1) use of a model factor (ISO, 2013) and (2) allowance for uncertainty by appropriate selection of a partial factor for resistance (ISO, 2013).

3.3 Resistance in sand

3.3.1 Drained versus undrained resistance

The mechanical behaviour of sand may be drained, partially drained or undrained. The actual drainage conditions for an element of sand depend on factors such as the duration of the load, the geometry of a suction bucket, and the permeability of the sand. Soil behaviour for sustained loads, such as self-weight of the structure is usually drained. Soil behaviour for (cyclic) environmental loads, such as waves is usually undrained, or partially drained. For example for waves, the drainage period is usually

N	F/F_{max}	$\tau_{cy,1}/\sigma'_{vc}$	$\tau_{cy,2}/\sigma'_{vc}$	$\tau_{cy,3}/\sigma'_{vc}$
1	100	0.100	0.150	0.200
2	95	0.095	0.143	0.190
4	88	0.088	0.132	0.176
8	81	0.081	0.122	0.162
15	74	0.074	0.111	0.148
30	67	0.067	0.101	0.134
50	59	0.059	0.089	0.118
90	51	0.051	0.077	0.102
200	41	0.041	0.062	0.082
500	23	0.023	0.035	0.046

$\tau_{cy,1}/\sigma'_{vc}$, $\tau_{cy,2}/\sigma'_{vc}$, and $\tau_{cy,3}/\sigma'_{vc}$ are arbitrarily chosen normalised shear stress ratios to calculate the locus of end points in Fig. 14

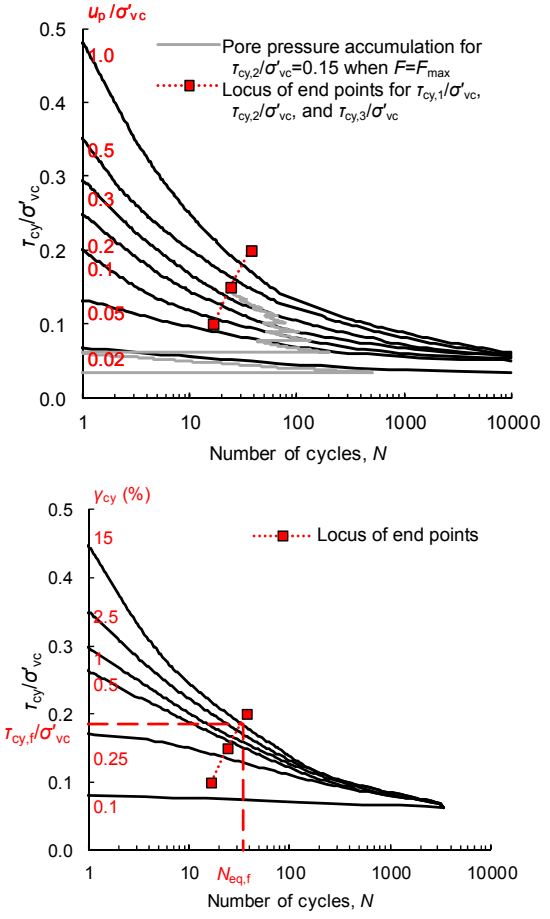

Fig. 14 Pore pressure accumulation procedure. Adapted from (Andersen, 2015), Copyrights 2015, with permission from Taylor & Francis

(a) Cyclic pore pressure u_p (kPa) contour diagram; (b) Cyclic shear strain γ_{cy} (-) contour diagram

equal to a multiple of the wave period. Hence, the immediate response to wave loads is undrained. The excess pore pressures generated during a wave will dissipate during subsequent waves.

3.3.2 Drained resistance

In compression, the drained capacity of a suction caisson in dense to very dense sand is usually very large. However in tension, only friction on the outside and inside of the skirt is available, which is usually limited. The drained compressive resistance can be calculated using standard limit equilibrium solutions. Eqs. (3) and (4) can be used for estimation of skirt friction in tension, where the selection of parameter values for coefficient of lateral pressure K (-) should take into account the effect of the installation method.

3.3.3 Undrained and partially drained resistance

The compressive capacity of a suction foundation in sand is usually smaller for the undrained case than for the drained case (assuming top plate bearing), especially if cyclic degradation occurs.

For rapid tensile loading, suction caisson design can cautiously assume fully drained conditions. However, during sufficiently rapid tensile loading, partially drained to undrained conditions can apply for relatively large suction buckets (Houlsby et al., 2005; Tjelta, 2015). Important factors for partially drained or undrained resistance of sand are: (1) time load history; (2) rate of loading; (3) coefficient of consolidation of the soil; (4) cyclic resistance of the soil; (5) caisson geometry; (6) distance to drainage boundary (e.g. seafloor).

Fig. 15 illustrates the load-bearing behaviour of a suction bucket in dense sand for different rates for tensile loading. With increased loading rate, the soil behaves more undrained. It can be seen that the undrained and partially drained tensile capacities are much larger than for the drained case. This is because of suction underneath the caisson lid creating an additional resistance. Note that this requires the suction caisson to be sufficiently watertight during the design life, so that suction pressures inside the caisson can be achieved.

The undrained cyclic resistance of a suction caisson depends on the static mean (drained) load (e.g. self-weight) on the caisson. A higher mean load (i.e. higher vertical effective stress), leads to higher cyclic undrained shear strength. However, the mean vertical effective stress during a storm may also be in tension for one or more suction caissons of an offshore structure. This design case may for example apply to relatively light weight structures with

relatively high overturning, semi-permanent moments (e.g. due to wind loads), such as tripods and jackets used typically in the wind industry. This setting will reduce the cyclic undrained shear strength.

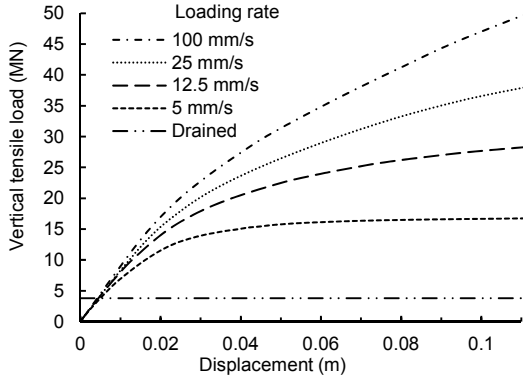

Fig. 15 Influence of loading rate on load-bearing behaviour. Adapted from (Whyte et al., 2017), Copyrights 2017, with permission from Society for Underwater Technology, London

Dense to very dense sands, above the critical state line, will dilate when sheared. For undrained conditions, such increase in volume cannot occur (as water is virtually incompressible). This implies that the undrained shear strength is basically limited by the shear stress where dilation will eventually occur due to the pore pressure exceeding the vacuum pressure or due to a phase change from dissolved gas (possibly present in the pore water) into free gas.

For loose to medium dense sands, below the critical state line, shearing will lead to contractive volume change. If the pore water cannot dissipate (i.e. undrained conditions) this will lead to a reduction of the effective stress and related reduction of undrained shear strength. This can ultimately lead to foundation failure.

The method presented by Andersen (2015) can be used to assess the cyclic resistance of a suction foundation in sand. This method considers that the pore pressures generated by a load parcel under undrained conditions will dissipate (partially) from the start of that parcel and continue to dissipate during subsequent load parcels. Hence, the cumulative excess pore pressure is lower than the excess pore pressure for fully undrained conditions. The Hansteen (1981) approach assumes the load parcels to be in an increasing order, with the second largest load cycles just before the largest load cycles. A more advanced approach would be to run a real design storm, cycle by cycle, through a τ_{cy}/σ'_{vc} versus N diagram. This approach offers benefits when the largest cycle is preceded by much smaller waves and when the second largest (wave) cycle is a significant period away from the largest cycle. This is usually the case. The longer period between the second largest and largest cycle allows intermediate dissipation of excess pore pressure generated by the second largest cycle. Hence, the excess pore pressures generated by the second largest cycle will have (partially) dissipated before the largest cycle will occur. This procedure leads to less cumulative pore pressure build-up and hence less cyclic damage than the Andersen (2015) method.

It is important to cautiously assess the dissipation time, when allowing for (partial) pore pressure dissipation. This requires coverage of a sufficient time period of the storm for generating a cautious pore pressure build-up before the largest cycle occurs. A sufficient time period is achieved when adding an additional time period does not significantly change the calculated pore pressure build-up anymore.

Fig. 16 illustrates the importance of cautious assessment of dissipation time for tensile capacity during cyclic loading of a suction foundation. Starting from the fully drained soil behaviour (on the right hand side of Fig. 16), the tensile capacity is equal to the drained skirt friction. Moving to the left, the soil behaviour becomes partially drained, and some suction may develop underneath the top lid, creating additional resistance. Moving further, the maximum tensile capacity is reached when the loading conditions during one cycle are fully undrained, and full drainage of excess pore pressures occurs during a limited number of cycles, so that only limited cyclic soil strength degradation and pore water pressure build-up will occur. However, when moving further to the left, it will take more and more cycles to fully drain the soil, leading to more cyclic degradation and pore pressure build-up. Ultimately on the left side of Fig. 16, soil behaviour is fully undrained. The coefficient of consolidation significantly affects the drainage behaviour. The soil coefficient of consolidation can usually only be assessed with an uncertainty in the order of one magnitude in laboratory tests. The coefficient of consolidation also varies with changes in effective stress and is usually anisotropic,

where the vertical coefficient of consolidation c_v (m^2/s) is usually lower than the horizontal coefficient of consolidation c_h (m^2/s). This introduces a significant uncertainty in the assessment of the soil drainage behaviour and related cyclic tensile capacity.

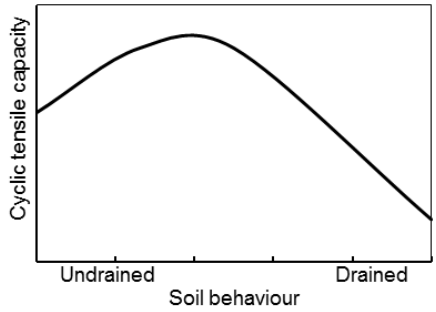

Fig. 16 Soil strength in relation to soil drainage behaviour

Andersen (2015) presented contour plots of permanent pore pressure as a function of cyclic shear stress and number of cycles in laboratory DSS tests on normally consolidated, reconstituted sand and silt specimens (Fig. 17). Some of the plots show an increase in u_p/σ'_{ref} with an increase of τ_{cy}/σ'_{ref}, where u_p is the accumulated pore pressure (kPa) and σ'_{ref} is the reference stress (kPa). This may not be representative of actual soil behaviour. Cyclic DSS tests usually simulate undrained conditions. No back pressure is applied and the test specimen may not be fully saturated. The simulation is achieved by allowing no volume change during the test (i.e. axial strain close to 0%). This is done by changing the axial stress while shearing during the test (Dyvik et al., 1987). When densely compacted, sand has a high stiffness. This means the DSS apparatus must be very stiff and very well controlled to maintain a situation of no volume change, which is extremely difficult in practice. Small axial strains may actually have occurred during the tests at higher cyclic stress levels, possibly causing erroneous results. For example, assume a cyclic DSS test at an initial axial stress of 200 kPa, a constrained modulus M of 15 MPa, and an axial strain of 0.4% during cyclic shear loading (Fig. 18). To compensate for the measured axial strain of −0.2% to 0.4%, the load needs to be corrected by approximately −30 kPa to 60 kPa, which is 30% of the initial axial stress. This will have a significant effect on the pore pressure build-up, the number of cycles to failure, and hence the interpreted pore pressure contour diagram. For the specific type of DSS apparatus used for the cyclic DSS test of Fig. 18, it will have led to an increased number of cycles to failure and an over prediction of the cyclic shear strength in design.

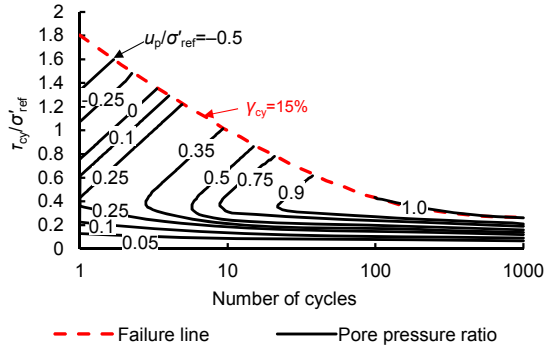

Fig. 17 Contour plots of permanent pore pressures for dense sand derived from DSS tests. Adapted from (Andersen, 2015), Copyrights 2015, with permission from Taylor & Francis

$\sigma'_{ref}=p_a(\sigma'_{vc}/p_a)^{0.9}$, σ'_{vc} is the vertical effective consolidation stress, and p_a is the atmospheric pressure (100 kPa)

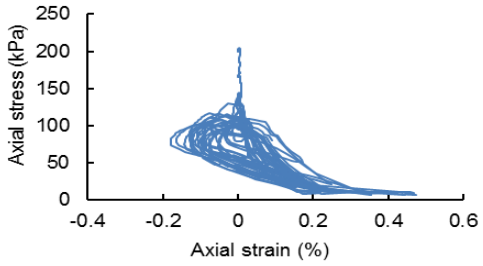

Fig. 18 Example of axial strain measured in cyclic DSS (Courtesy of Statoil)

Another issue is the representativeness and uncertainty of results from laboratory cyclic tests on reconstituted sand specimens compared to in situ soil conditions:

1. The estimation of the density of a sample, to simulate in situ soil conditions. This is usually done by estimating the relative density from CPT correlation and minimum/maximum density testing. Blaker et al. (2015) illustrated difficulties with minimum/maximum density testing and related large variation in test results between different test methods.

2. The lateral stress conditions which are uncontrolled in a DSS test.

3. The effects of aging, which are likely to be absent in the reconstituted sample.

4. The effects of pre-cycling, which may (or may not) have been done for a limited number of cycles, compared to thousands of cycles in reality.

The author is not aware of literature providing recommendations on how to account for differences between reconstituted samples and in situ soil conditions for prototype suction caissons. For suction caisson design, consultation of a geotechnical expert could be considered to address this issue.

4 Suction foundation serviceability

4.1 Types of displacement

The following types of displacements can be distinguished: (1) Displacements induced by elastoplastic shear stress response; (2) Consolidation settlements; (3) Post cyclic reconsolidation settlements; (4) Ratcheting.

4.2 Displacements induced by elastoplastic shear stress response

Structural analysis typically requires input in the form of stiffness matrices, describing the deformation and rotations that occur for the load cases considered. Fig. 19 presents a stiffness matrix, where T is the torsional moment (kNm), G is the shear modulus of soil (kPa), u is the horizontal displacement (m), w is the vertical displacement (m), θ is the moment rotation (rad), ω is the torsional rotation (rad), R is the caisson radius (m), and K_V, K_H, K_{MH}, K_{HM}, K_M, and K_T are dimensionless elastic stiffness coefficients (-), which only depend on Poisson's ratio v (-) and embedment depth ratio d/R, where d is the embedment depth (m).

For preliminary design, stiffness matrices can be derived using recommendations by Doherty and Deeks (2003) or Doherty et al. (2005), if the skirt is relatively flexible. For detailed design, stiffness matrices are often assessed using FEM modelling, where the structural model and geotechnical model are usually uncoupled. Integrated soil-structure analysis can also be considered (Erbrich et al., 2016).

A stiffness matrix implies elastic conditions. This differs from reality, where elastoplastic behaviour and hysteresis are observed. The elastoplastic nature of the soil causes the stiffness matrices to be stress dependent.

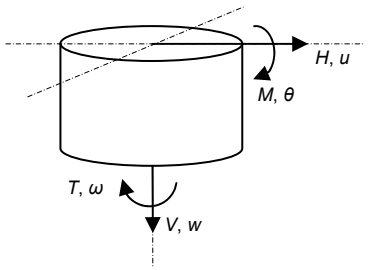

$$\begin{bmatrix} V/(GR^2) \\ H/(GR^2) \\ M/(GR^3) \\ T/(GR^3) \end{bmatrix} = \begin{bmatrix} K_V & 0 & 0 & 0 \\ 0 & K_H & K_{HM} & 0 \\ 0 & K_{MH} & K_M & 0 \\ 0 & 0 & 0 & K_T \end{bmatrix} \begin{bmatrix} w/R \\ u/R \\ \theta \\ \omega \end{bmatrix}$$

Fig. 19 Stiffness matrix

An important parameter in the stiffness matrix is the shear modulus of the soil. The shear modulus varies with shear strain and loading conditions (e.g. monotonic or cyclic loading), as can be seen in Fig. 20. For fatigue analysis and dynamic response, usually the small strain shear modulus G_0 (kPa) is used. For higher (first time) loads, stiffness degradation occurs due to elastoplastic deformation. Subsequent unload/reload stiffness usually is much stiffer than the first time loading stiffness. If the structural model and geotechnical model are uncoupled, an iterative procedure is usually adopted for detailed design, whereby the stiffness matrices are reviewed and, if required, updated based on the results of structural analysis.

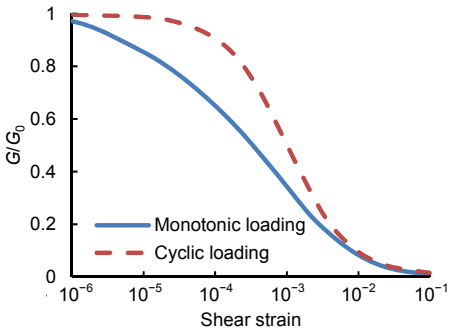

Fig. 20 Shear modulus versus shear strain for monotonic and cyclic loading. Adapted from (Mayne, 2001), Copyrights 2001, with permission from the author

4.3 Consolidation settlements

Consolidation settlements occur in clay due to sustained loading (e.g. self-weight) of the suction foundation and if present, the superstructure. Primary

consolidation settlements can be calculated using 1D consolidation theory (Terzaghi and Fröhlich, 1936). Secondary consolidation can be calculated using the theory originally developed by Keverling Buisman (1940) and afterwards refined into the concept of isotachs (Yin and Graham, 1996). Consideration must be given to the influence of skirt friction (Section 3.2) and top plate (caisson lid) bearing.

4.4 Post cyclic reconsolidation settlements

Excess pore pressures, generated by cyclic loading conditions will lead to additional consolidation of sand and clay layers. These post cyclic reconsolidation settlements can be significant. Post cyclic reconsolidation settlements can be estimated by detailed FEA pore pressure accumulation analysis. In preliminary design, the post cyclic reconsolidation settlements can be estimated based on approximate calculations by a geotechnical expert.

4.5 Ratcheting

Suction foundations in sand and subject to cyclic loading, require design checks for ratcheting. Ratcheting can lead to both uplift and settlements. Fig. 21 shows model tests on cyclically loaded caissons showing ratcheting settlements.

A suction bucket can gradually ratchet into the soil or out of the soil due to cyclic non-recoverable plastic deformations that are primarily drainage induced. The deformations heavily depend on loading rate and coefficient of consolidation. Ratcheting analysis requires fully coupled consolidation-deformation FEA, capturing the correct stress-dilatancy behaviour. Whyte et al. (2017) reviewed constitutive models available in commercial FEA software and found them generally unsuitable. For example, when using the dilatancy angle in the standard Mohr Coulomb (MC) model, in undrained conditions, a critical state condition will never be reached, resulting in infinite undrained shear strength. According to Whyte et al. (2017) there have been significant advances in constitutive modelling over the last few decades, with a vast number of advanced models proposed by various research groups, such as Taiebat and Dafalias (2008). However, industry uptake of such models is rare. This may be related to numerical instabilities, slow runtimes, difficulties in calibration of (often) numerous model parameters, and lack of availability in commercial FEA software packages.

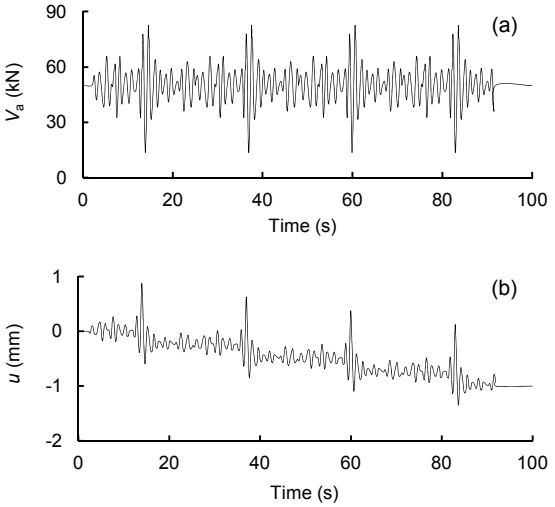

Fig. 21 Model tests showing ratcheting-type displacements: (a) vertical action v_a versus time; (b) vertical displacement u versus time

Adapted from (Houlsby, 1999), Copyrights 1999, with permission from the author

Whyte et al. (2017) presented a simple constitutive model, called the Fugro Dilational Model. This model represents a slight adaptation on a model presented by Erbrich (1994). It captures the soil stress-dilatancy response with a simple versatile state-dependent plastic potential and it includes a cavitation cut off. Fig. 22 shows an example axisymmetric FEA calculation of a suction caisson in dense sand subjected to two axial load parcels consisting of a number of small cyclic loads followed by a significantly larger load cycle. The average load is close to zero. The selected convention is positive for tensile loading and upward displacement. As can be seen, each large load cycle results in a small permanent additional upward displacement of approximately 6 mm, whereas the smaller load cycles do not result in significant additional displacement and are mainly elastic. The small permanent displacements will accumulate under a full storm distribution. Such ratcheting can lead to unacceptable displacements and related tilt or even failure of the structure.

Whyte et al. (2017) performed similar 3D FEA for combined axial and two-component horizontal cyclic loads acting on a single suction foundation of multi-pod structure, considering a realistic full storm history. At the load levels investigated, these analyses showed that the horizontal loads had only a minor influence on the axial ratcheting displacement of the

bucket during partially drained conditions. Therefore, an axisymmetric model considering only the vertical loading from a storm history may be considered adequate for capturing partially drained ratcheting behaviour.

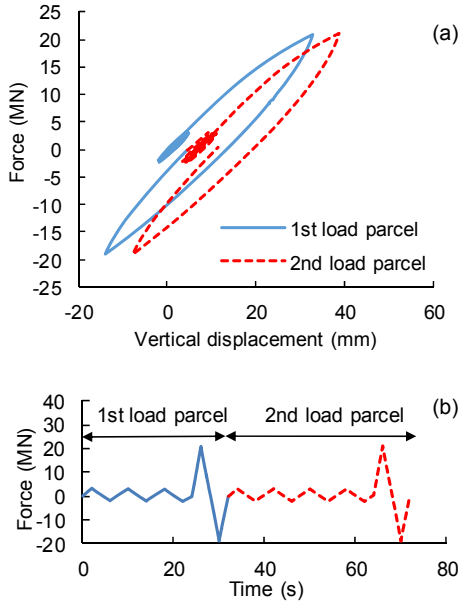

Fig. 22 Suction caisson response to cyclic loading showing ratcheting effect
(a) Force displacement diagram; (b) Force time diagram

5 Suction caisson extraction feasibility

Two situations may be considered for suction caisson extraction feasibility:

1. Suction caisson retrieval during the installation phase. For example, retrieval may be necessary because of excessive tilt. Another installation attempt is then necessary.

2. Suction caisson removal at the end of operations. For example, removal may be necessary for structure relocation or decommissioning.

The extraction feasibility assessment is comparable to the installation feasibility assessment. Differences are:

1. Extraction is achieved by applying overpressure inside the caisson, instead of suction. In sand, this will lead to an increase in effective stress inside the caisson and a reduction of the effective stress outside the caisson. High overpressures may lead to base failure in clay and piping in sand. In both cases it may not be feasible to extract the suction caisson.

2. Skirt resistance will typically increase over time (time effects). Time effects can be significant during suction caisson removal and, to a lesser degree, for suction caisson retrieval.

3. Reversed end-bearing may apply to the skirt annulus in clay, adding to the extraction resistance.

4. The self-weight of the caisson and superstructure reduce the required suction pressure during the installation phase. During the extraction phase they will counter-act and increase the required overpressure.

5. The void between the top plate and seafloor may have been grouted (under base grouting).

6. A crane may provide additional force to help retrieve the suction caisson; however, the crane capacity may be small compared to the extraction resistance.

Extraction by applying overpressure inside caissons has been successfully carried out in a number of projects. An example of successful extraction is the relocation of three multi-purpose platforms in the Dutch Sector of the North Sea. The platforms were operated by Wintershall and equipped with four suction caissons. The platforms were first installed at the end of the last millennium and relocation took place in 2000, 2001, and 2013 (SPT Offshore, 2017).

Acknowledgements

The author gratefully acknowledges the support and commitment granted by Fugro, the Netherlands.

References

Allersma HGB, Hogervorst JR, Pimoulle M, 2001. Centrifuge modelling of suction pile installation in layered soil by percussion method. Proceedings of OMAE'01: 20th International Conference on Offshore Mechanics and Arctic Engineering, Paper No. OMAE2001/OFT-1036.

Andersen KH, 2015. Cyclic soil parameters for offshore foundation design. Frontiers in Offshore Geotechnics III: Proceedings of the Third International Symposium on Frontiers in Offshore Geotechnics (ISFOG 2015), CRC Press, USA.

Andersen KH, Jostad HP, Dyvik R, 2008. Penetration resistance of offshore skirted foundations and anchors in dense sand. *Journal of Geotechnical and Geoenvironmental Engineering*, 134(1):106-116. https://doi.org/10.1061/(ASCE)1090-0241(2008)134:1(106)

Begemann HK, 1976. The influence of excavation on soil strength below excavation level. Sixth European Conference on Soil Mechanics and Foundation Engineering, Deep Foundations and Deep Excavations, p.613-616.

Bhattacharjee S, Majhi SM, Smith D, et al., 2014. Serpentina FPSO mooring integrity issues and system replacement:

unique fast track approach. Proceedings OTC 2014: Offshore Technology Conference, OTC Paper 25449.

Blaker Ø, Lunne T, Vestgården T, et al., 2015. Method dependency for determining maximum and minimum dry unit weights of sands. Frontiers in Offshore Geotechnics III: Proceedings of the Third International Symposium on Frontiers in Offshore Geotechnics (ISFOG 2015).

Brinch Hansen J, 1970. A revised and extended formula for bearing capacity. *The Danish Geotechnical Institute Bulletin*, 28:5-11.

Broug NWA, 1988. The effect of vertical unloading on cone resistance QC, a theoretical analysis and a practical confirmation. Proceedings of the 1st International Geotechnical Seminar on Deep Foundations on Bored and Auger Piles, p.523-530.

Colliard D, Wallerand R, 2008. Design and installation of suction piles in West Africa deepwaters. Proceedings of the Second British Geotechnical Association International Conference on Foundations (ICOF 2008), Volume 1: Piles, Excavations and Offshore Foundations, p.825-836.

DNV (Det Norske Veritas), 2005. DNV-RP-E303 Geotechnical Design and Installation of Suction Anchors in Clay. DNV, Norway.

DNV (Det Norske Veritas), 2017. DNVGL-RP-C212 Offshore Soil Mechanics and Geotechnical Engineering. DNV GL AS, Norway.

Doherty JP, Deeks AJ, 2003. Elastic response of circular footings embedded in a non-homogeneous half-space. *Géotechnique*, 53(8):703-714. https://doi.org/10.1680/geot.2003.53.8.703

Doherty JP, Houlsby GT, Deeks AJ, 2005. Stiffness of flexible caisson foundations embedded in nonhomogeneous elastic soil. *Journal of Geotechnical and Geoenvironmental Engineering*, 131(12):1498-1508. https://doi.org/10.1061/(ASCE)1090-0241(2005)131:12(1498)

Dyvik R, Berre T, Lacasse S, et al., 1987. Comparison of truly undrained and constant volume direct simple shear tests. *Géotechnique*, 37(1):3-10. https://doi.org/10.1680/geot.1987.37.1.3

Erbrich CT, 1994. Modelling of novel foundation for offshore structures. Proceedings of the 9th UK ABAQUS User's Conference, p.235-251.

Erbrich CT, Tjelta TI, 1999. Installation of bucket foundations and suction caissons in sand—geotechnical performance. 31st Annual Offshore Technology Conference, OTC Paper 10990.

Erbrich CT, Wallbridge P, Yamamoto N, 2016. Numerical modelling of seismically induced settlement for Ichthys Riser Support Structure. Offshore Technology Conference Asia, OTC Paper 26778.

Feld T, 2001. Suction Buckets, a New Innovative Foundation Concept, Applied to Offshore Wind Turbines. PhD Thesis, Aalborg University, Denmark.

Gylland AS, de Vries MH, 2008. The effect of gas blow-out on shallow offshore foundations. Proceedings of the Second British Geotechnical Association International Conference on Foundations (ICOF 2008), Volume 1: Piles, Excavations and Offshore Foundations, p.885-896.

Hansteen OE, 1981. Equivalent Geotechnical Storm, Report 4007-4016. Norwegian Geotechnical Institute, Norway.

Houlsby GT, 1998. Caisson foundations for offshore foundations on sand. A Two Day International Conference on Subsea Geotechnics.

Houlsby GT, 1999. Suction caisson foundations for offshore structures: performance under cyclic loading. Seabed Geotechnics, 2nd Annual Conference.

Houlsby GT, Byrne BW, 2005a. Design procedures for installation of suction caissons in clay and other materials. *Proceedings of the Institution of Civil Engineers-Geotechnical Engineering*, 158(GE2):75-82.

Houlsby GT, Byrne BW, 2005b. Design procedures for installation of suction caissons in sand. *Proceedings of the Institution of Civil Engineers-Geotechnical Engineering*, 158(GE3):135-144.

Houlsby GT, Kelly RB, Byrne BW, 2005. The tensile capacity of suction caissons in sand under rapid loading. Proceedings of the First International Symposium on Frontiers in Offshore Geotechnics, p.405-410.

Ibsen LB, Thilsted CL, 2010. Numerical study of piping limits for installation of large diameter buckets in layered sand. The European Conference on Numerical Methods in Geotechnical Engineering, p.921-926.

ISO (International Organization for Standardization), 2013. Petroleum and Natural Gas Industries-General Requirements for Offshore Structures, ISO 19900:2013. ISO, Switzerland.

ISO (International Organization for Standardization), 2016. Petroleum and Natural Gas Industries Specific Requirements for Offshore Structures, Part 4: Geotechnical and Foundation Design Considerations, ISO 19901-4:2016. ISO, Switzerland.

Kay S, 2013. Torpedo piles—VH capacity in clay using resistance envelope equations. Proceedings of the 32nd International Conference on Ocean, Offshore and Arctic Engineering.

Kay S, Palix E, 2010. Caisson capacity in clay: VHM resistance envelope—Part 2: VHM envelope equation and design procedures. Frontiers in Offshore Geotechnics II: Proceedings of the 2nd International Symposium on Frontiers in Offshore Geotechnics, p.741-746.

Kay S, Palix E, 2011. Caisson capacity in clay: VHM resistance envelope—Part 3: extension to shallow foundations. ASME 2011 30th International Conference on Ocean, Offshore and Arctic Engineering, Paper No. OMAE2011-49077.

Keverling Buisman AS, 1940. Grondmechanica. Waltman, Delft, the Netherlands (in Dutch).

Kolk HJ, Kay S, Kirstein A, et al., 2001. North Nemba flare bucket foundations. Offshore Technology Conference, OTC Paper No. 13057.

Lee YC, Audibert JME, Tjok KM, 2005. Lessons learned from several suction caisson installation projects in clay. Proceedings of the First International Symposium on Frontiers in Offshore Geotechnics, p.235-241.

Mayne PW, 2001. Stress-strain-strength-flow parameters from enhanced in-situ tests. Proceedings of the International Conference on In Situ Measurement of Soil Properties and Case Histories, p.27-47.

Murff JD, Hamilton JM, 1993. *P*-ultimate for undrained analysis of laterally loaded piles. *ASCE Journal of Geotechnical Engineering*, 119(1):91-107. https://doi.org/10.1061/(ASCE)0733-9410(1993)119:1(91)

O'Neil M, Erbrich C, McNamara A, 2018. Prediction of seabed trench formation induced by anchor chain motions. Offshore Technology Conference, OTC Paper No. OTC-29068-MS.

Panagoulias S, van Dijk BFJ, Drummen T, et al., 2017. Critical suction pressure during installation of suction caissons in sand. Offshore Site Investigation & Geotechnics, Proceedings of the 8th International Conference, p.570-577.

Senders M, Randolph M, 2009. CPT-based method for the installation of suction caissons in sand. *Journal of Geotechnical and Geoenvironmental Engineering*, 135(1): 14-25. https://doi.org/10.1061/(ASCE)1090-0241(2009)135:1(14)

Senders M, Randolph M, Gaudin C, 2007. Theory for the installation of suction caissons in sand overlaid by clay. Offshore Site Investigation and Geotechnics, Proceedings of the 6th International Conference, p.429-438.

Senpere D, Auvergne GA, 1982. Suction anchor piles–a proven alternative to driving or drilling. Proceedings of the 14th Offshore Technology Conference, OTC Paper No. 4206.

SPT Offshore, 2017. Wintershall Multi Purpose Platform. http://www.sptoffshore.com/en/track-record1/detail/wintershall-multi-purpose-platform

Standards Norway, 2007. NORSOK Standard N-003: Actions and Action Effects, 2nd Edition. Norsok, Lysaker.

Taiebat M, Dafalias YF, 2008. SANISAND: simple anisotropic sand plasticity model. *International Journal for Numerical and Analytical Methods in Geomechanics*, 32:915-948.

Terzaghi K, 1943. Theoretical Soil Mechanics. John Wiley & Sons, USA.

Terzaghi K, Fröhlich OK, 1936. Theorie der Setzung von Tonschichte. Deuticke, Germany (in German).

Tjelta TI, 2015. The suction foundation technology. Frontiers in Offshore Geotechnics III: Proceedings of the Third International Symposium on Frontiers in Offshore Geotechnics (ISFOG 2015).

Tran MN, Randolph MF, 2008. Variation of suction pressure during caisson installation in sand. *Géotechnique*, 58(1): 1-11. https://doi.org/10.1680/geot.2008.58.1.1

Tran MN, Randolph MF, Airey DW, 2005. Study of seepage flow and sand plug loosening in installation of suction caissons in sand. Proceedings of ISOPE-05, 15th International Conference on Offshore Mechanics and Arctic Engineering, Paper No. 2005-JSC-137.

Tran MN, Randolph MF, Airey DW, 2007. Installation of suction caissons in sand with silt layers. *Journal of Geotechnical and Geoenvironmental Engineering*, 133(10): 1183-1191. https://doi.org/10.1061/(ASCE)1090-0241(2007)133:10(1183)

van Dijk BFJ, 2015. Caisson capacity in undrained soil: failure envelopes with internal scooping. Frontiers in Offshore Geotechnics III: Proceedings of the 3rd International Symposium on Frontiers in Offshore Geotechnics, p.337-342.

Watson PG, Gaudin C, Senders M, et al., 2006. Installation of suction caissons in layered soil. Proceedings of the Sixth International Conference on Physical Modelling in Geotechnics, p.685-691.

Whyte S, Rattley M, Erbrich C, et al., 2017. A practical constitutive model for soil structure interaction problems involving dense sands. Offshore Site Investigation Geotechnics, Proceedings of the 8th International Conference, p.400-407. https://doi.org/10.3723/OSIG17.400

Yin JH, Graham J, 1996. Elastic visco-plastic modelling of one-dimensional consolidation. *Géotechnique*, 46(3): 515-527. https://doi.org/10.1680/geot.1996.46.3.515

中文概要

题　目： 吸力式基础设计

目　的： 吸力式基础具有投资费用低、施工时间短、无噪音和可重复使用等优点，因此被广泛应用在海洋工程领域。本文针对吸力式基础设计中的关键问题，主要综述现有设计理论，指出理论缺陷，并给出设计建议。

创新点： 综述砂土、粘土和成层土中吸力式基础的安装、回收、基础承载力、基础沉降和服役性能中的关键科学问题和现有设计理论。

方　法： 1. 基于文献报道的现场试验和模型试验，针对吸力式基础安装过程中的沉贯阻力、临界吸力和土塞效应，评估现有设计理论的准确性；2. 分析粘土和砂土中吸力式基础的完全排水、完全不排水和部分排水条件下静力和循环承载力计算理论；3. 针对吸力式基础的长期服役性能，分析荷载引起的基础变形、固结沉降、循环再固结沉降和极端荷载下的“棘轮效应”。

结　论： 1. 现有的吸力式基础安装中沉贯阻力计算理论没有普适性；对于临界吸力的计算，由于没有考虑“土拱效应”，理论计算值均低估了安装吸力。2. 对于粘土中吸力式基础承载力的计算需要考虑循环作用下土体的强度弱化和基础-土间空隙引起的承载力降低，而砂土中基础承载力计算需要考虑排水条件的影响。3. 对于吸力式基础的长期服役性能，特别是基础变形的计算，目前还缺少成熟的计算理论。

关键词： 吸力式基础；安装；承载力；变形